To Appear in ApJ January 10, 1997

The Nature of the X-Ray Emission and the Mass Distributions in Two Early-Type Galaxies

David A. Buote[1] and Claude R. Canizares
Department of Physics and Center for Space Research 37-241,
Massachusetts Institute of Technology
77 Massachusetts Avenue, Cambridge, MA 02139,
buote@ast.cam.ac.uk, crc@space.mit.edu

ABSTRACT

We present spectral analysis of *ASCA* observations of the early-type galaxies NGC 720 (E4) and NGC 1332 (E7/S0) with emphasis on constraining the relative contribution to the X-ray emission from hot gas and the integrated emission from X-ray binaries. Single-temperature spectral models yield poor fits to the spectrum ($\chi^2_{red} \sim 3$) over the $\sim 0.5 - 5$ keV energy range. Two-temperature models significantly improve the spectral fits ($\chi^2_{red} \sim 1.5$) and have soft-component temperatures and sub-solar abundances consistent with previous *ROSAT* single-temperature models ($T_{soft} \sim 0.6$ keV, abundances ~ 0.1) and hard-component temperatures ($T_{hard} \gtrsim 3$ keV) consistent with those expected from a discrete component. The soft component dominates the emission in both galaxies, especially in the 0.4 - 2.4 keV band used in previous *ROSAT* studies: flux ratios are $F_{hard}/F_{soft} = 0.19(0.16 - 0.45)$ for NGC 720 (2σ) and $F_{hard}/F_{soft} = 0.31(0.24 - 0.55)$ for NGC 1332 (90%). Combining these spectral results with *ROSAT* data we updated constraints on the mass distributions for NGC 720 and NGC 1332. For NGC 720, which yields the more precise constraints, the ellipticity of the intrinsic shape of the mass is slightly reduced ($\Delta\epsilon_{mass} \approx 0.05$) when the discrete component is added, $\epsilon_{mass} \sim 0.4 - 0.6$ (90%). The estimates for the total mass increase with increasing discrete flux, and we find that models with $F_{hard}/F_{soft} = 0.45$, the 2σ upper limit, have masses that exceed by $\sim 30\% - 50\%$ those where $F_{hard}/F_{soft} = 0$.

Subject headings: galaxies: elliptical and lenticular, cD – galaxies: fundamental parameters – galaxies: individual (NGC 720, NGC 1332) – galaxies: structure – X-rays: galaxies

---

[1]Present Address: Institute of Astronomy, Madingley Road, Cambridge CB3 0HA, UK

1. Introduction

It is well known that the hot, X-ray–emitting gas in many early-type galaxies is one of the best probes of the mass distributions in these systems (e.g., Binney & Tremaine 1987; Fabbiano 1989). However, it is also well known that the X-ray emission is of a more complex origin than a single-phase isothermal hot gas in hydrostatic equilibrium (e.g., Canizares, Fabbiano, & Trinchieri 1987; Kim, Fabbiano, & Trinchieri 1992; Pellegrini & Fabbiano 1994; Eskridge, Fabbiano, & Kim 1995). Although the relative importance of cooling flows and supernovae winds in the hot gas has received much attention and remains a controversial topic (e.g., Thomas 1986; Canizares et al. 1987; Loewenstein & Mathews 1987; David, Forman, & Jones 1990; Ciotti et al. 1991; Rangarajan 1995), the contribution to the total X-ray emission from the integrated emission from X-ray binaries (e.g., Canizares et. al. 1987; Kim et al. 1992), and in particular, the effect of such a discrete component on determinations of the mass distributions of early-type galaxies, has received comparatively less attention

We have previously analyzed in detail the mass distributions of the early-type galaxies NGC 720 (E4) and NGC 1332 (E7) using X-ray data from the *ROSAT* (Trümper 1983) satellite (Buote & Canizares 1994, 1996a, 1996c; hereafter BCa, BCb, and BCc). The relatively large ratio of X-ray to blue-band optical luminosity (L_X/L_B) for NGC 720 suggests that the hot gas dominates the X-ray emission (Canizares et al. 1987; Kim et al. 1992), though NGC 1332, which has a smaller value of L_X/L_B, may contain a significant fraction of discrete emission. By assuming the X-rays are due only to hot gas in hydrostatic equilibrium, we constrained the intrinsic shapes of the gravitating matter distributions to have ellipticities $\epsilon_{mass} \sim 0.5 - 0.7$ for NGC 720 and $\epsilon_{mass} \sim 0.3 - 0.8$ for NGC 1332 at the estimated 90% confidence levels; the total masses of both galaxies were $\sim 10^{12} M_{\odot}$ assuming an isothermal gas. For NGC 1332, however, we (in BCb) also considered a model for the emission from discrete sources which was spatially distributed like the optical light. We found that the lower limit on ϵ_{mass} decreased when the relative fraction of discrete emission to hot-gas emission was increased; however, the derived total masses increased. Unfortunately, the *ROSAT* Position Sensitive Proportional Counter (PSPC) data had insufficient spectral resolution to place useful constraints on the relative contribution to the emission from a discrete component and hot-gas component.

In this paper we present spectral analysis of data for NGC 720 and NGC 1332 obtained by the *ASCA* satellite (Tanaka, Inoue, & Holt 1994). With its superior spectral resolution over *ROSAT*, and its sensitivity to energies above 3 keV, the *ASCA* data allow the relative fraction of the discrete emission and hot-gas emission to be measured much more precisely than in the previous studies. We combine these new results with the previous *ROSAT* data to obtain updated constraints on the mass distributions in these galaxies. In §2 we describe the observations and reduction of the *ASCA* data; in §3 we present the spectral analysis; in §4 we update the mass distributions using both the *ASCA* and *ROSAT* data; finally, in §5 we present our conclusions.

2. Observations and Data Analysis

NGC 720 was observed on July 17-18, 1993 as part of the Performance Verification (PV) phase for a nominal exposure of 40 ks, and NGC 1332 was observed on August 5-6, 1995 as part of the Guest Observation (GO) phase AO3 for a nominal exposure time of 60 ks. We focus on the data taken with the two Solid-State Imaging Spectrometers (SIS) because of their superior spectral resolution compared to the Gas Imaging Spectrometers (GIS). Moreover, our primary focus is to measure the relative importance of a soft and hard component, as well as the temperature and abundances of the soft ($\sim$ 1 keV) component that is due to hot gas emitting thermal bremsstrahlung. We found that the SIS data provided the best constraints on spectral models and that incorporating the GIS data did not significantly improve the constraints on the spectral model parameters. We mention that Matsushita et al. (1994) have found that the GIS is more effective than the SIS for analyzing the hard ($\gtrsim$ 3 keV) emission in early-type galaxies.

Because of the size of the point spread function (PSF) of the ASCA X-ray Telescope (XRT) (Takahashi et al. 1995), the spatial distributions of the X-ray emission of NGC 720 and NGC 1332 are essentially those of point sources. Considering the asymmetry of the XRT, ongoing calibration uncertainties, and relatively low signal-to-noise ratio, S/N, of the observations, detailed spatial analysis of these point-like sources is inappropriate, and we will concentrate our attention on the spectral properties of the X-ray data.

For the observation of NGC 720 the SIS were configured in 4-CCD mode, bright data mode, and high bit rate. Since NGC 720 is point-like, the principal advantage of using 4-CCD mode is to obtain a reliable estimate of the local background. Fortunately, the sensitivity of 4-CCD mode had not yet degraded substantially due to radiation damage (Dotani, Yamashita, & Rasmussen 1995) at the time of the PV-phase observation of NGC 720. However, because of the degradation of the SIS at the time of AO3, the configuration for the NGC 1332 observation was set to single-CCD mode with faint data mode and medium bit rate.

To prepare each SIS observation for spectral analysis we (1) screened the data to create a cleaned event list, (2) determined the aperture extraction radius which optimized S/N, and (3) extracted the source and background spectra. All of the reduction procedures were implemented using the standard XSELECT, FTOOLS, and IRAF-PROS software packages. See Day et al. (1996) for a description of the standard *ASCA* data reduction and analysis procedures.

We screened the SIS data using the FTOOLS routine *ascascreen*. For NGC 720, we set the minimum elevation angle (ELV) from the Earth for SIS0 to 15°, a slightly more stringent value than the standard 10°, and relaxed the SIS1 to $ELV = 5°$. The other screening parameters were kept at their standard values, though we did have to manually set the pixel rejection threshold to 100; we also used an intermediate value for the Radiation Belt Monitor threshold ($RBM = 250$). For NGC 1332 we found that the standard settings for the screening parameters worked well (with RBM and pixel rejection threshold as above). The resulting filtered exposure times for NGC 720 are 32.0 ks (SIS0) and 33.9 ks (SIS1), and for NGC 1332 we obtained 53.6ks (SIS0) and 53.1 ks

(SIS1).

Next for each SIS we determined the size of the spatial aperture that optimized S/N. NGC 1332 was placed at the default position for a point source in single-CCD mode; i.e. $\sim 5'$ along the diagonal from where the corners of the 4 SIS chips meet on chip 1 for the SIS0, chip 3 for the SIS1. Since the PSF is asymmetrical, it is difficult to precisely define the center of this relatively low S/N source; so we simply selected a center by eye. We then computed the counts (with photons in all available energies) in circular apertures of different radii. (We used circular apertures rather than an elliptical aperture more closely resembling the shape of the PSF, because the procedure to obtain auxiliary response files (ARFs), $ascaarf$, which accounts for the effective area due to the XRT and window absorption, currently performs best on circular regions.)

In choosing a region to compute the background we had to weigh the following considerations: the background region should be (1) far enough away from the source so as not to be contaminated by the galactic emission, (2) large enough to contain enough photons to reduce statistical noise, and (3) located as close as possible to the same region of the CCDs spanned by the source since vignetting effects are not accounted for in the ARFs. From these considerations we selected the background region to be an annulus ($r = 41 - 46$ pixels, or $r = 4.4' - 4.9'$), its center slightly shifted toward the center of the chip with respect to the adopted galaxy center in order to fit entirely on the chip. We found that the S/N was optimized for radii $r = 25$ and 20 pixels $(2.7', 2.1')$ for the SIS0 and SIS1 respectively.

Unfortunately NGC 720 was not positioned at the default position for a point source. Rather, the center was placed very near the gap between chips 1 & 2 for SIS0 and chips 3 & 0 for SIS1, almost $6'$ from where the corners of the 4 SIS chips meet on chip 1 for the SIS0, chip 3 for the SIS1. As a result, significant flux was lost in the gap between the chips. Again we centered by eye a circular aperture on NGC 720 and computed the counts for different radii. The aperture lay mostly on chips 1 & 3 for the SIS0 and SIS1 respectively, but some of the area covered respectively chips 2 & 0 as well. The gap was excluded from the circles. The background was estimated from two circular regions of radius $r = 2'$, one placed near the top left corner of chip 1 (3) and the other near the top right corner chip 2 (0) for the SIS0 (SIS1) in order to stay as far away from the galaxy as possible while remaining on the same chips. We found that the S/N was optimized for radii $r = 40, 32.5$ pixels $(4.3', 3.5')$ for the SIS0 and SIS1 respectively.

Finally, we extracted the spectra for the source and background. In addition to the local background, we also computed the background from the deep exposures of regions of "blank sky" provided from the $ASCA$ Guest Observer Facility (GOF); we used the November 1994 versions of these observations. An advantage of using the blank sky observations is that their spectra may be computed from the same region of the CCDs as the source and thus telescopic vignetting, which is not accounted for by the ARF files, will be the same for both source and background. Also, being deep exposures the blank sky templates have the background level determined more precisely with regards to photon statistics. The principal problem with the blank sky templates is that the

cosmic X-ray background varies with position on the sky.

3. Spectral Analysis

The SIS spectrum spans the energy range 0.4 - 12 keV and, in Bright mode, consists of 2048 Pulse Invariant (PI) bins which have been corrected for exposure and instrument variations over the SIS. Upon extraction, each SIS spectrum is automatically rebinned into 512 PI channels to improve S/N. We further rebinned the PI channels so that each bin had at least 40 and 50 counts for NGC 720 and NGC 1332 respectively. We used PV-phase redistribution matrices (RMFs) (version 0.8) provided by the *ASCA* Team at the *ASCA* GOF for NGC 720 and generated our own epoch-dependent (version 0.9) RMFs for NGC 1332 using the FTOOLS package *sisrsp*. The RMFs specify the channel probability distribution for photons of a given energy; i.e. the response matrix (RSP) is the product of the ARF (§2) and the RMF.

Because of current calibration uncertainties (*ASCA* GOF 1996), we do not analyze PI bins with energies $E \leq 0.5$ keV. Since the X-ray emission from early-type galaxies is generally very weak for $E \gtrsim 8$ keV (e.g., Awaki et al. 1994; Matsushita et al. 1994), we also neglect those high-energy bins in our fits. Our motivation for this is to reduce the systematic effects due to the background spectrum, which dominates at those energies. Also, the contribution from foreground and background sources will be most serious at those energies where the S/N of the galactic emission is low.

We present the background-subtracted SIS spectra for NGC 720 in Figure 1 and for NGC 1332 in Figure 2. The background-subtracted count rates are given in Table 1. The blank-sky templates are used as our standard for the background estimates, though for comparison all of the ensuing analysis was also performed using the local background estimates. For N1332, the count rates are essentially consistent for both background estimates. For NGC 720 the blank sky templates are systematically larger than the local values by $\sim 20\%$. However, the results from spectral fitting are quite consistent when either the blank sky template or local background is used.

As the purpose of this investigation is to understand the relative contribution to the X-ray emission from hot gas and discrete sources, we first fitted the spectra to thermal models having a single temperature. (BCc and BCb have shown that the ROSAT PSPC data rules out single-component discrete models for NGC 720 and NGC 1332). Then we fitted two-temperature models to the spectra to investigate whether the fits are improved over single-temperature models. All of the spectral fitting was performed with XSPEC.

We present the results of the spectral fits in Table 2 and Figures 1 and 2. The results listed in Table 2 all have the Hydrogen column density, N_H, fixed to the galactic value as determined by Stark et al. (1992); $N_H = (1.4, 2.2) \times 10^{20}$ cm^{-2} for respectively NGC 720 and NGC 1332. We found that in all of the fits the value of χ^2_{red} remained essentially unchanged when N_H was allowed

to vary and was always consistent with the Galactic value.

The count rates for the SIS0 exceed those of the SIS1 for both galaxies because of the greater sensitivity of the SIS0. However, because of the greater sensitivity the extraction region used for the SIS0, and thus the flux, is slightly larger than that of the SIS1. For NGC 720 in particular, the models generally lie slightly below the data for the SIS0 and slightly above the data for the SIS1. The extraction regions differ by only about $r \sim 1'$, which is smaller than the PSF. Since the properties of the galaxies should not change drastically over those scales this should not pose a serious problem in the interpretation of joint fitting of the SIS0 and SIS1 data.

The single-temperature (1T) models give very poor fits for both galaxies because they cannot account for the emission above $E \sim 3$ keV. The Raymond-Smith (RS) models, which yield the best fits, have best-fit temperatures and abundances that are marginally consistent with previous determinations from the ROSAT PSPC (BCa,BCb,BCc), which probed the energy range 0.1 - 2.4 keV. We do not give confidence levels for the 1T models because of the poor fits.

The SIS spectra compel us to consider more complex models, of which a natural extension are two-temperature (2T) models. We present results for the RS models, where we required the abundances of each temperature component to be the same in the fits. Thus, we have four interesting parameters: T_{soft}, Abun, T_{hard}, and the relative normalization of the two components. We express this last parameter as F_{hard}/F_{soft}, the ratio of the fluxes of the two components in the 0.4 - 2.4 keV band.

As shown in Table 2 and Figures 3 and 4, the 2T models provide much better fits to the spectra. Although the quality of the fits, as given by $\chi^2_{red} \sim 1.5 - 1.7$, is not formally acceptable, considering the simple assumptions of the RS models (i.e. single-phase thermal line spectrum) over the large energy range $E \sim 0.5 - 5$ keV, the 2T RS models would seem to be a good qualitative description for our purposes; i.e. to determine the relative contribution to the emission from a hard and soft component. The estimated 1σ and 2σ ($\Delta\chi^2 = 4.72, 9.70$) confidence levels are given for NGC 720, while we list 1σ and 90% ($\Delta\chi^2 = 4.72, 7.78$) levels for NGC 1332; only 90% confidence is given for NGC 1332 because the lower S/N does not allow constraints on the upper limit for the abundances at 2σ which is important for determining the lower limit on F_{hard}/F_{soft}.

For both galaxies the best-fit values and confidence ranges are very similar for the parameters T_{soft}, Abun, and T_{hard}, with the values for NGC 720 determined somewhat more precisely due to the higher S/N. The values for $T_{soft} \sim 0.6(0.5 - 0.7)$ keV and the sub-solar abundances are consistent with previous 1T models determined from the ROSAT PSPC for these galaxies (BCa,BCb,BCc) as expected because of the 0.1 - 2.4 keV pass band of ROSAT. However, both galaxies clearly require a second, high-temperature component ($T_{hard} \gtrsim 5$ keV), that is consistent with the integrated emission from X-ray binaries (i.e. discrete sources) in the galaxies (Canizares et al. 1987; Kim et al. 1992). Using the *Einstein* results from Canizares et al. (1987), the approximate expected 0.5 - 4.5 keV flux due to the emission from discrete sources is $\sim 1.6 \times 10^{-13}$ erg cm^{-2} s^{-1} for NGC 720 and $\sim 1.3 \times 10^{-13}$ erg cm^{-2} s^{-1} for NGC 1332, which are in reasonable

agreement with the fluxes in Table 1.

In order to compare to previous *ROSAT* results for NGC 720 and NGC 1332, we list in Table 2 the values for F_{hard}/F_{soft} in the energy band 0.4 - 2.4 keV; this band is also the principal band of emission for hot gas with $T \sim 1$ keV. The SIS spectra provide interesting constraints on the relative fluxes of the two components and demonstrate that the soft component in both galaxies, which is probably due to hot gas, dominates the total X-ray emission in the 0.4 - 2.4 keV band. As expected, the soft component constitutes a larger fraction of the total 0.4 - 2.4 keV emission in NGC 720 because of its larger ratio of X-ray to optical blue-band luminosity, L_X/L_B, than NGC 1332 (Kim et al. 1992). Over the 0.5 - 5 keV band, however, the hard component becomes more important, though it does not dominate the total emission in either galaxy: $F_{hard}/F_{soft} = 0.40(0.36 - 0.59)(0.35 - 0.73)$ for 1σ and 2σ respectively for NGC 720, and $F_{hard}/F_{soft} = 0.65(0.52 - 0.96)(0.52 - 1.02)$ for 1σ and 90% respectively for NGC 1332. For clarity, the individual values of F_{soft} and F_{hard} are listed in Table 1 for both the 0.4 - 2.4 keV and 0.5 - 5 keV bands. The values of F_{hard}/F_{soft} are comparable both when the background is taken from the sky templates and the local estimates.

The qualitative properties of the two spectral components for NGC 720 and NGC 1332 are similar to previous *ASCA* analyses of a small sample of early-type galaxies in Virgo (Awaki et al. 1994; Matsushita et al. 1994). There are, however, some notable differences. The inferred lower limits on T_{hard} derived in this paper generally exceed those determined for the Virgo galaxies. This difference would not appear to be due to larger uncertainties for the Virgo galaxies because their count rates are factors of 5-10 larger than for NGC 720 and NGC 1332. This result is consistent with the values of T_{hard} of the Virgo galaxies being diminished because of a contribution from the diffuse cluster emission ($T \sim 2$ keV, as suggested by Matsushita et al. 1994), whereas NGC 1332, and especially NGC 720, do not reside in regions of high galaxy density. This contamination from the diffuse cluster gas may also account for the $\sim 25\%$ larger values of T_{soft} of the Virgo galaxies in comparison to NGC 720 and NGC 1332.

Although the abundances for NGC 1332 are not tightly constrained, NGC 720 has precisely determined RS abundances that are slightly lower than found for the bright Virgo ellipticals NGC 4406, NGC 4472, and NGC 4636 studied by Awaki et al. (1994) and Matsushita et al. (1994), but are consistent with those of NGC 1404 and NGC 4374 (Loewenstein et al. 1994). We advise caution in interpreting the precise values of the abundances as a result of the marginal fits of the RS models; i.e. the residuals below 2 keV are suggestive of line emission that is not well accounted for by the models, which would raise the abundances to some degree. See, e.g., Loewenstein et al. (1994), for a discussion of the implications of these low abundances for models of the origin of the hot gas.

It is interesting to compare the values of F_{hard}/F_{soft} for NGC 720 with NGC 4472 (similarly for NGC 1332 with NGC 4374) because the galaxies have similar values of L_X/L_B (Kim et. al. 1992). Awaki et al. (1994) obtained $F_{hard}/F_{soft} = 0.09(0.04 - 0.15)$ (90% confidence) in the 0.5

- 4.5 keV band for NGC 4472 which is substantially smaller than for NGC 720. In contrast, the luminosities of the hard components of NGC 4472 and NGC 720 agree to within $\sim 20\%$. Although the fluxes of both NGC 720 and NGC 4472 are dominated by the soft component for 0.4 - 2.4 keV, the precise values, as well as those in the broader bands, have distinctly different values. This suggests that although L_X/L_B is a useful indicator for when the hot gas dominates the X-ray emission, the specific flux ratio of the hot gas and emission from discrete sources clearly depends on other factors; e.g., the environment of the galaxies.

4. Implications for the Mass Distributions

We now consider the effects of the *ASCA* spectral results on the mass distributions in NGC 720 and NGC 1332. The uncertainty associated with the temperature profile of the hot gas in an early-type galaxy is generally the principal limiting factor in the accuracy for determining the mass distribution assuming hydrostatic equilibrium (e.g., Binney & Tremaine 1987; Fabbiano 1989). The spatial resolution of *ASCA* is inadequate for measuring the radial temperature profiles for NGC 720 and NGC 1332. Spatial (polytropic) and spectral analysis of *ROSAT* PSPC data indicate a nearly isothermal gas for NGC 720 (BCa), though for NGC 1332 the temperature profile is less certain (BCb). The temperature profiles in other early-type galaxies have been found to be very nearly isothermal (e.g., Forman et. al. 1993; David et al. 1994; Trinchieri et al. 1994; Kim & Fabbiano 1995; Rangarajan et al. 1995).

For an isothermal gas the gravitating mass is directly proportional to the gas temperature and thus the superior spectral resolution of *ASCA* should provide more robust constraints than the previous PSPC studies. However, single-temperature spectral models fitted the PSPC spectrum quite well for NGC 720 and NGC 1332 (BCa, BCb, BCc), whereas the *ASCA* data requires two components (and thus two more free parameters). As a result, the precision of the constraints on the soft component of the *ASCA* data turns out to be similar to the single-temperature values obtained with the PSPC data. Hence, the mass distributions of NGC 720 and NGC 1332 are not substantially clarified by the new determinations of the temperatures in this paper (see below).

Unlike with the temperature, the *ASCA* data give a significantly more precise description of F_{hard}/F_{soft} than in previous *ROSAT* studies (BCb, BCc) which does affect the determination of the shape of the mass profile and the total amount of gravitating mass. Here we update our previous work for NGC 720 and NGC 1332 incorporating the new temperatures and abundances for the soft component, which we assume is due to emission from hot gas, and the relative fluxes from the hot gas and hard component, which we take to be directly proportional to the optical light; for detailed explanations of our modeling procedures see BCa and BCc for NGC 720 and BCb for NGC 1332.

4.1. NGC 720

We recomputed the shape of the total gravitating matter in NGC 720 and revised our estimate of its total mass. Our analysis combined the PSPC and High Resolution Imager (HRI) (David et al. 1995) data so that the mass models (see below) satisfied both data sets simultaneously. The X-ray radial profiles for the HRI and PSPC data and the ellipticities of the HRI data are as described in BCc. However, because our data analysis techniques have evolved since BCa, we obtained more precise 68% and 90% confidence levels on the X-ray ellipticities for the PSPC data using the Monte Carlo procedure described in BCc; the technique for computing the ellipticities is explained in §2.1.2 of BCa. The results are listed in Table 3. For semi-major axis $a = 90''$ (which was used to constrain the mass shape in BCa), the 90% lower limit on the ellipticity is smaller (0.15) than computed by BCa (0.20), though the upper limit is the same. However, as we show below, the derived limits on the mass shape are actually very similar because the HRI data (BCc) gives 90% confidence lower limits on the ellipticity for $a \sim 90\%$ that agree with the values determined by BCa. In this present study we found that the lower limits on the HRI data for $a \sim 50'' - 90''$ and the new upper limits on the PSPC data for $a \sim 60'' - 75''$ provided the important constraints on the mass models.

As it is our principal goal to explore the effects of the new spectral constraints derived in this paper, particularly with respect to F_{hard}/F_{soft}, we have focused our attention on a restricted set of models. First, we take the gas to be isothermal which is a good assumption for NGC 720 (BCa), a more uncertain one for NGC 1332 (BCb). Second, we assume that each galaxy is viewed edge-on. Third, we ignore the position angle twist of the X-ray isophotes in NGC 720 (BCc). Finally, we assume a spheroidal mass distribution (SMD), where the mass density is stratified on concentric, similar spheroids; note that if the X-ray position-angle twist is due to the projection of a triaxial mass distribution, then the oblate and prolate spheroidal models should bracket the possible aggregate triaxial shapes and masses. We take the density run to be given by a power-law with slope -2, $\rho_{mass} \sim (a_c^2 + a^2)^{-1}$, where a_c is a core radius. BCa showed that models with steeper slopes do not fit the data as well. We have also found that the following results do not change qualitatively if we choose models without a core, like the generalized Hernquist (1990) models used in Buote & Canizares (1996b). As in our previous studies, we fixed the semi-major axis of the boundary of the mass spheroid to $450''$ ($43.6h_{80}^{-1}$ kpc assuming a distance of $20h_{80}^{-1}$ Mpc for both NGC 720 and NGC 1332).

We list the results for the shape of the total gravitating mass in Table 4. For $F_{hard}/F_{soft} = 0$ the ellipticity of the mass is $\epsilon_{mass} \sim 0.45 - 0.65$ at 90% confidence, essentially as we found in BCa. The upper limit on ϵ_{mass} does not change much for $F_{hard}/F_{soft} = 0.16, 0.19$, although the lower limit is reduced by ~ 0.08. As expected, the most extreme behavior is observed for $F_{hard}/F_{soft} = 0.45$ where the lower limit on ϵ_{mass} falls by ~ 0.20, and the upper limit by ~ 0.10. These results imply that for the most probable values of F_{hard}/F_{soft} obtained from the *ASCA* data, $\epsilon_{mass} \sim 0.4 - 0.6$, which would appear to be in good agreement with the elongation of the flattest, most extended optical isophotes for NGC 720 ($\epsilon \sim 0.45$) and the globular cluster system

(Kissler-Patig, Richtler, & Hilker 1995).

The total gravitating masses of these models are listed in Table 5. The masses are not a strong function of F_{hard}/F_{soft}, though there is a trend of larger masses for larger values of F_{hard}/F_{soft}. This results because the discrete component, which follows the optical light, is very centrally concentrated (Lauer et al. 1995), while the X-rays are considerably more extended (core radius $\sim 15''$). Thus, to compensate for a greater fraction of the emission being distributed like the optical light, the hot-gas model must become even more extended which translates to more mass since the asymptotic mass density slope is fixed at -2.

The derived masses for $F_{hard}/F_{soft} = 0.16, 0.19$ exceed by $\sim 15\%$ those for $F_{hard}/F_{soft} = 0$, while the $F_{hard}/F_{soft} = 0.45$ masses are $\sim 30\% - 50\%$ higher than for $F_{hard}/F_{soft} = 0$. It is clear that to obtain the most precise constraints on the masses of elliptical galaxies it is important to consider the spatial distribution of the discrete component. Here we have assumed it is distributed like the optical light, but it would be better to determine this directly from the X-ray observations, which is not possible with *ASCA*. We mention that the derived gas mass for NGC 720 is in good agreement with the PSPC determination of BCa, though we now have some extra uncertainty due to the range of F_{hard}/F_{soft}: $M = 8.3(5.7 - 10.1)h_{80}^{-5/2} \times 10^9 M_\odot$ (2σ).

4.2. NGC 1332

Unfortunately, NGC 1332 presented some complications when incorporating the discrete component into the formalism. Unlike NGC 720, the "core" of the X-ray emission of NGC 1332 is not clearly resolved by the PSPC, and we found the width of the PSPC PSF to be uncertain at the off-axis position for NGC 1332 (BCb); i.e. the spatial distribution of the X-ray emission of NGC 1332 for radii $\lesssim 15''$ is quite uncertain. In BCb we considered mass models having, in addition to the hot gas, a discrete component that followed the optical light and found behavior very similar to that described above for NGC 720.

However, we have re-examined the results of BCb and have determined that the behavior of the hot gas + discrete models is quite sensitive to the uncertainties in the PSF (though the hot-gas only models are not, as shown in BCb). If the width of PSF is taken so that the core is resolved (as in BCb), then we obtain results as before. But, when the PSF width is increased so that the core is completely unresolved (appropriate to the off-axis position of NGC 1332 – see BCb), then we find different behavior. In this case, because the X-ray core is unresolved, the core of the mass model must decrease as the proportion of the discrete model is increased to compensate for the extended (albeit centrally concentrated) discrete model.

Because of this ambiguity, which requires higher spatial resolution X-ray data (e.g., HRI) to resolve, we refrain from presenting new shape and mass estimates for NGC 1332 analogous to NGC 720. Instead we have computed the mass for NGC 1332 using the new temperatures and abundances, but we use the hot-gas-only models from BCb. We use the same type of mass model

as for NGC 720 and find: $M = (0.74 - 1.28)(0.62 - 1.46)h_{80}^{-1} \times 10^{12} M_{\odot}$ for respectively 68% and 90% confidence levels for oblate models and similarly $M = (0.53 - 1.02)(0.41 - 1.27)h_{80}^{-1} \times 10^{12} M_{\odot}$ for prolate models. As expected, these masses agree quite well with the previous determinations in BCb; the gas masses using the new spectral results are essentially unaltered from the results of BCb.

5. Conclusions

Our joint analysis of new *ASCA* data and *ROSAT* data for NGC 720 and NGC 1332 clearly shows the existence of a hard component, but the soft component dominates the emission in both of the galaxies. Using the *ASCA* SIS data we obtained in the 0.4 - 2.4 keV band appropriate to previous *ROSAT* studies, $F_{hard}/F_{soft} = 0.19(0.16 - 0.45)$ for NGC 720 (2σ) and $F_{hard}/F_{soft} = 0.31(0.24 - 0.55)$ for NGC 1332 (90%), where F_{hard}/F_{soft} is the relative flux of the hard and soft components. The larger values of F_{hard}/F_{soft} for NGC 720 are consistent with the notion that a larger value of L_X/L_B is related to the relative importance of the hot gas with respect to emission from discrete sources (Kim et al. 1992).

We have explored the effects of a discrete component on the mass distributions of NGC 720 and NGC 1332. The estimates of the ellipticity of the mass distribution are only slightly reduced when taking into account a reasonable contribution from a discrete component; the revised ellipticities taking into account the emission from discrete sources do not systematically exceed the ellipticity of the flattest optical isophotes ($\epsilon \sim 0.45$). The derived mass of NGC 720 increases as F_{hard}/F_{soft} increases. We have thus found that to obtain the most precise constraints on the masses of elliptical galaxies it is important to consider the spatial distribution of the discrete component. Here we have assumed it is distributed like the optical light, but it would be better to determine this directly from the X-ray observations, which is not possible with *ASCA*, but will be with *AXAF*.

We gratefully acknowledge the kind help of K. Arnaud and K. Mukai for patiently answering questions regarding the reduction of *ASCA* data. This research was supported by grants NASGW-2681 (through subcontract SVSV2-62002 from the Smithsonian Astrophysical Observatory), and NAG5-2921.

Table 1: *ASCA* Count Rates and Fluxes

	Counts/s (10^{-2} s^{-1})		F_{soft} (10^{-13} erg cm^{-2} s^{-1})		F_{hard} (10^{-13} erg cm^{-2} s^{-1})		F_{total} (10^{-13} erg cm^{-2} s^{-1})	
Target	SIS0	SIS1	SOFT	BROAD	SOFT	BROAD	SOFT	BROAD
720:								
SKY	4.3 ± 0.14	2.6 ± 0.11	5.9(4.5-6.5)	5.4(4.3-5.8)	1.1(1.0-2.0)	2.2(2.0-3.1)	7.0(6.5-7.6)	7.6(7.4-7.9)
LOCAL	3.8 ± 0.16	2.3 ± 0.12	5.2(3.5-6.0)	4.9(3.5-5.4)	0.8(0.6-1.9)	1.6(1.3-2.8)	6.0(5.4-6.6)	6.5(6.2-6.7)
1332:								
SKY	1.6 ± 0.07	0.9 ± 0.06	2.7(2.0-3.2)	2.5(2.0-2.8)	0.8(0.8-1.1)	1.6(1.6-2.1)	3.5(3.1-4.0)	4.2(4.1-4.4)
LOCAL	1.6 ± 0.09	0.9 ± 0.07	2.7(1.8-3.3)	2.5(1.8-2.8)	0.9(0.9-1.3)	1.7(1.7-2.3)	3.5(3.1-4.2)	4.2(4.1-4.6)

Note. — SKY and LOCAL refer to whether the background is subtracted using the blank sky templates or from a portion of the observed field. The count rates are for energies $E > 0.5$ keV. The quantities F_{soft}, F_{hard}, and $F_{total} = F_{soft} + F_{hard}$ refer to the fluxes determined from two-temperature models in §3. The SOFT and HARD columns refer to pass bands 0.4 - 2.4 keV and 0.5 - 5 keV respectively. The listed values of the fluxes are for the best fit values and 2σ/90% uncertainties for NGC 720 and NGC 1332 respectively.

Table 2. Results of Spectral Fits

	T_{soft} (keV)		Abun (% Solar)		T_{hard} (keV)	F_{hard}/F_{soft} (0.4 - 2.4 keV)		χ^2	χ^2_{red}
NGC 720									
1-T Models									
RS	0.68	···	0.05	···	···	···	···	144	2.7
MEWE	0.54	···	0.00	···	···	···	···	259	4.9
MEKA	0.58	···	0.07	···	···	···	···	162	3.1
2-T Models									
RS 1σ	0.64	0.58 - 0.68	0.08	0.05 - 0.14	≥ 5.3	0.19	0.17 - 0.34	77	1.5
RS 2σ	0.64	0.54 - 0.70	0.08	0.04 - 0.21	≥ 3.5	0.19	0.16 - 0.45	77	1.5
NGC 1332									
1-T Models									
RS	0.77	···	0.10	···	···	···	···	96	3.3
MEWE	0.50	···	0.00	···	···	···	···	157	5.1
MEKA	0.57	···	0.07	···	···	···	···	119	4.0
2-T Models									
RS 1σ	0.63	0.51 - 0.69	0.14	0.06 - 0.71	≥ 6.7	0.31	0.24 - 0.52	48	1.7
RS 90%	0.63	0.47 - 0.70	0.14	0.05 - 3.02	≥ 4.8	0.31	0.24 - 0.55	48	1.7

Note. — The notation for the spectral models (as they appear in XSPEC) is RS for Raymond & Smith (1977, updated to current version), MEWE for Mewe, Gronenschild, & van den Oord (1985), and MEKA for an amended version of MEWE due to Kaastra (1992). Confidence ranges for the 2-T models were determined assuming 4 interesting parameters.

Table 3: Revised PSPC Ellipticities for NGC 720

a (arcsec)	ϵ_X	68%	90%
60	0.10	0.08 - 0.19	0.06 - 0.23
75	0.21	0.15 - 0.23	0.12 - 0.25
90	0.25	0.18 - 0.28	0.15 - 0.30
105	0.24	0.18 - 0.30	0.10 - 0.33

Note. — Ellipticity of PSPC X-ray surface brightness as a function of semi-major axis (a) computed using the Monte Carlo procedure described in BCc.

Table 4: Updated Shape of the Gravitating Matter in NGC 720

F_{ds}/F_{hg}	Oblate ϵ_{mass}		Prolate ϵ_{mass}	
(%)	68%	90%	68%	90%
0	0.57-0.63	0.48-0.68	0.52-0.58	0.44-0.62
19	0.48-0.60	0.39-0.65	0.46-0.57	0.37-0.60
16	0.50-0.60	0.40-0.66	0.48-0.57	0.38-0.60
45	0.40-0.52	0.30-0.60	0.39-0.50	0.29-0.55

Note. — Hydrostatic mass models assuming the gas is isothermal following BCa. The $F_{ds}/F_{hg} = 0$ values represent the $\rho \sim r^{-2}$ mass density models of BCa revised using the HRI ellipticities in BCc and the PSPC ellipticities in Table 3.

Table 5: Updated Mass for NGC 720

	Mass ($10^{12} h_{80}^{-1} M_{\odot}$)			
F_{ds}/F_{hg}	Oblate		Prolate	
(%)	68%	90%	68%	90%
0	0.93-1.23	0.84-1.33	0.73-0.99	0.64-1.12
19	1.00-1.36	0.88-1.50	0.76-1.11	0.67-1.27
16	0.98-1.33	0.87-1.46	0.75-1.07	0.66-1.24
45	1.09 -1.55	0.95-1.76	0.87-1.32	0.74-1.54

Note. — These masses correspond to the models in Table 4 and the spectral results in Tables 1 and 2. The confidence limits are computed for a given value of F_{ds}/F_{hg}.

REFERENCES

ASCA GOF 1996, http://heasarc.gsfc.nasa.gov/docs/asca/dec95/siscal.html

Awaki, H. et al. 1994, PASJ, 46, L65

Binney, J., & Tremaine, S. 1987, Galactic Dynamics (Princeton: Princeton Univ. Press)

Buote, D. A., & Canizares, C. R. 1994, ApJ, 427, 86 (BCa)

Buote, D. A., & Canizares, C. R. 1996a, ApJ, 457, 177 (BCb)

Buote, D. A., & Canizares, C. R. 1996b, ApJ, 457, 565

Buote, D. A., & Canizares, C. R. 1996c, ApJ, in press (astro-ph/9601043) (BCc)

Canizares, C. R., Fabbiano, G., & Trinchieri, G. 1987, ApJ, 312, 503

Ciotti, L., Pellegrini, S., Renzini, A., & D'Ercole, A. 1991, ApJ, 376, 380

David, L. P., Forman, W., & Jones, C., 1990, ApJ, 359, 29

David, L. P., Harnden, F. R., Kearns, K. E., & Zombeck, M .V. 1995, The ROSAT High Resolution Imager (HRI), (U.S. ROSAT Science Data Center – Smithsonian Astrophysical Observatory)

David, L. P., Jones, C., & Forman, W. 1994, ApJ, 428, 554

Day, C., Arnaud, K., Ebisawa, K., Gotthelf, E., Ingham, J., Mukai, K., & White, N. 1996, The ABC Guide to *ASCA* Data Reduction, (GSFC: Greenbelt)

Dotani, T., Yamashita, A., & Rasmussen, A. 1995, ASCA News, 3, 25

Eskridge, P. B., Fabbiano, G., & Kim, D.-W. 1995, ApJS, 97, 141

Fabbiano, G. 1989, ARA&A, 27, 87

Forman, W., Jones, C., David, L., Franx, M., Makishima, K., & Ohashi, T. 1993, ApJ, 418, L55

Hernquist, L. 1990, ApJ, 356, 359

Kaastra, J. S. 1992, An X-ray Spectral Code for Optically Thin Plasmas (Internal SRON-Leiden Report, updated version 2.0)

Kim, D.-W., Fabbiano, G, & Trinchieri, G. 1992, ApJS, 80, 645

Kim, D.-W., & Fabbiano, G, 1995, ApJ, 441, 182

Kissler-Patig, M., Richtler, T., & Hilker, M. 1996, A&A, in press

Lauer, T. R., Ajhar, E. A., Byun, Y., Dressler, A., & Faber, S. M. 1995, AJ, 110, 2622

Loewenstein, M., & Mathews, W. G. 1987, ApJ, 319, 614

Loewenstein, M., et. al. 1994, ApJ, 436, L75

Matsushita, K., et. al. 1994, ApJ, 436, L41

Mewe, R., Gronenschild, E. H. B. M., & van den Oord, G. H. J. 1985, A&AS, 62, 197

Pellegrini, S., & Fabbiano G. 1994, ApJ, 429, 105

Rangarajan, F. V. N. 1995, Ph.D. Thesis, Cambridge University

Rangarajan, F. V. N., White, D. A., Ebeling, H., & Fabian, A. C. 1995, MNRAS, 277, 1047

Raymond, J. C., & Smith, B. W. 1977, ApJS, 35, 419

Stark, A. A., et al. 1992, ApJS, 79, 77

Tanaka, Y., Inoue, H., & Holt, S. S. 1994, PASJ, 46, L37

Takahashi, T., Markevitch, M., Fukazawa, Y., Ikebe, Y., Ishisaki, Y., Kikuchi, K., Makishima, K., Tawara, Y. 1995, ASCA News, 3, 34

Thomas, P. A. 1986, MNRAS, 220, 949

Trinchieri, G., Kim, D. W., Fabbiano, G., & Canizares, C., 1986, ApJ, 428, 555

Trümper, J. 1983, Adv. Space Res., 2, 241

Fig. 1.—
Reduced, background-subtracted SIS spectra for NGC 720 and the best-fit single-temperature RS model (dots) with the corresponding residuals = (model-data)/σ.

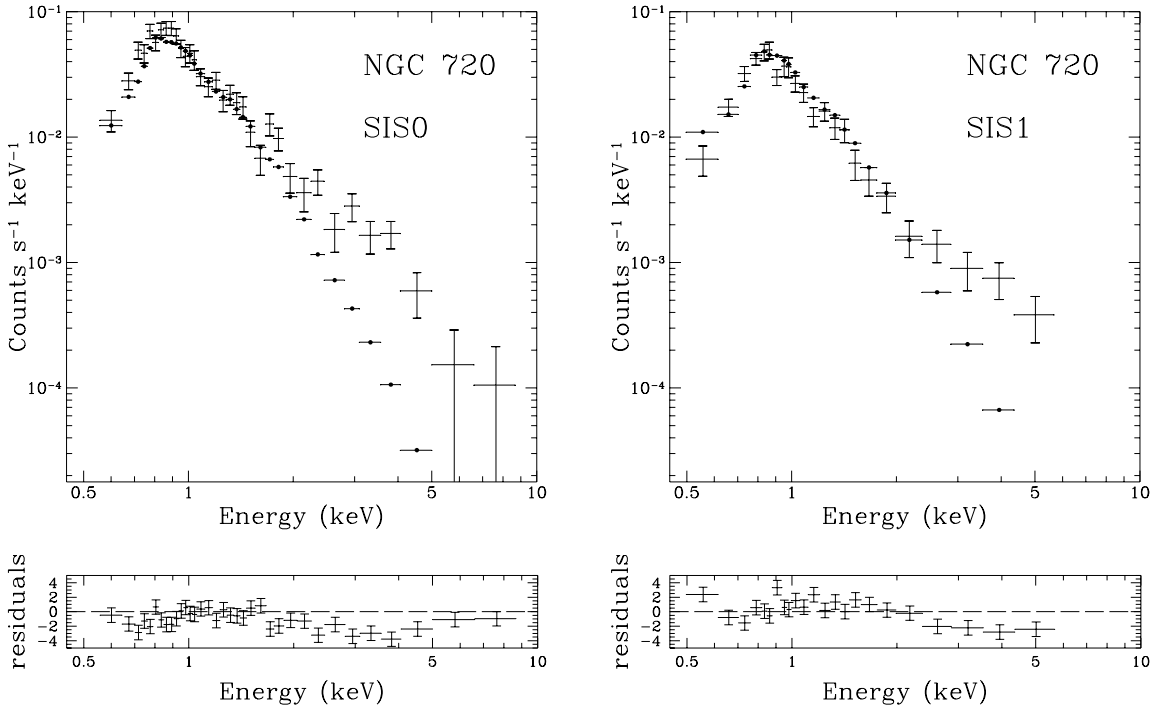

Fig. 2.—
Reduced background-subtracted SIS spectra for NGC 1332 and the best-fit single-temperature RS model (dots) with the corresponding residuals = (model-data)/σ.

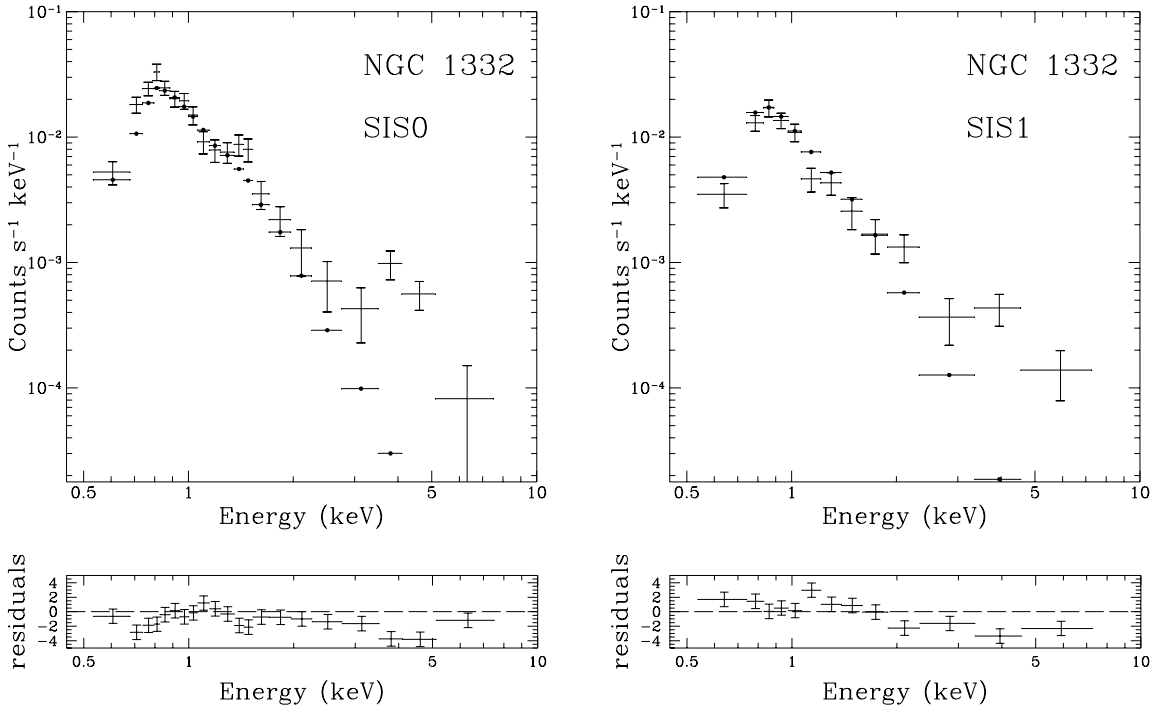

Fig. 3.—
Same as Figure 1 except dots are the best-fit two-temperature RS models.

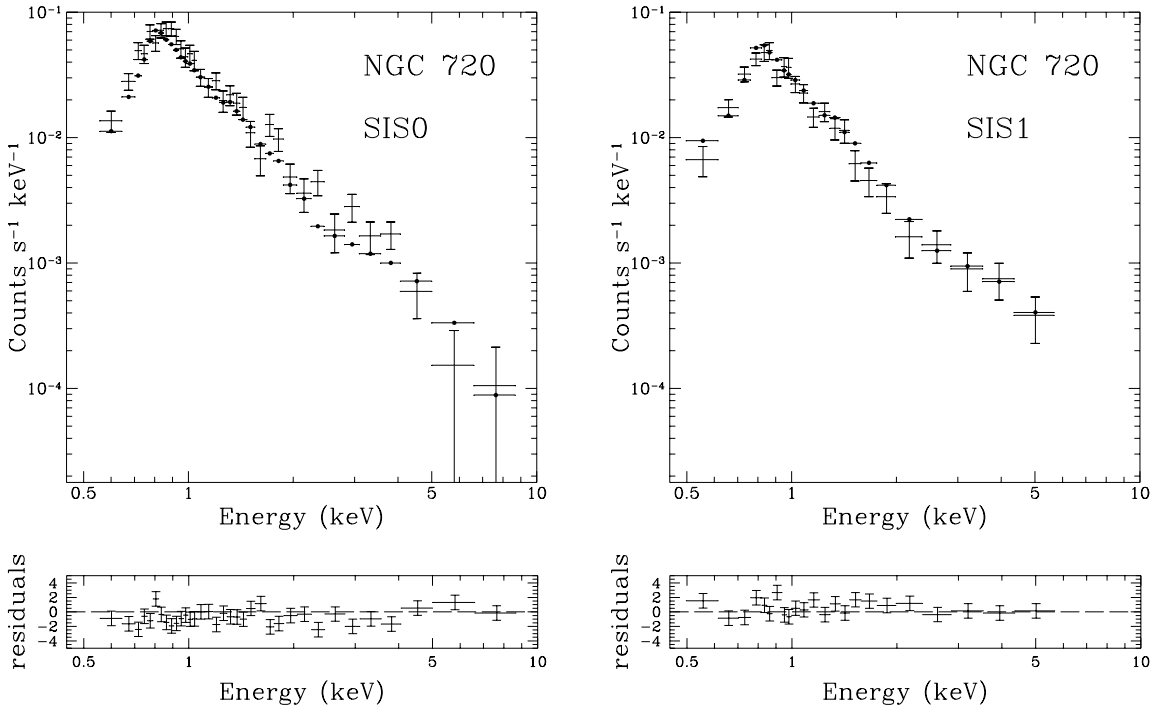

Fig. 4.—
Same as Figure 2 except dots are the best-fit two-temperature RS models.